PICTORIAL ESSAY MSK Imaging

Beaks and peaks in adult skeleton, Part II: Bony excrescences in lower extremity

Zehra Akkaya, Gülden Şahin
Ankara University, School of Medicine, Department of Radiology, Ankara, Turkey

SUBMISSION: 12/12/2019 | ACCEPTANCE: 14/3/2020

ABSTRACT

Bony protuberances are frequently seen in imaging of the adult skeleton. Congenital or acquired, some of these bony excrescences can be clues to the underlying disorder in the appropriate clinical context. It is important to know their imaging findings and typical location in order to establish an accurate diagnosis and have a grasp on their clinical significance. The first part of this review series covered the upper extremity and skull base. In this second part, we briefly describe common and clinically important bony excrescences in the lower extremity.

KEY WORDS

Deformity; Exostoses; Lower extremity; MR imaging; Radiography; Excrescences/osseous

Introduction

Bony protuberances in the adult skeleton may arise due to various reasons, including osteophyte and enthesophyte formations in chronic traction injuries, degenerative and inflammatory disorders, acquired or developmental abnormalities of the bone and congenital variations. The exact aetiology of these bony "bumps" is often not known.

When present, the most common symptom associated with such lesions is pain, which may arise secondary to friction and compressions of the adjacent tissues, bursa formation and internal derangement or inflammation of the joints if they have a juxta-articular location. Most of these lesions have characteristic imaging findings at typical anatomic sites, which may be an important clue to the underlying disorder.

CORRESPONDING AUTHOR, GUARANTOR

Zehra Akkaya,
Ankara University, School of Medicine, Department of Radiology, Keklikpinari mahallesi Dikmen caddesi 913. Sokak Turtaş Sitesi A-8 Blok No:14 Çankaya-Ankara, Turkey, Email: zehraakkaya@gmail.com

In the first part of this review series, (Akkaya Z, Çoruh AG, Şahin G. Beaks and peaks in adult skeleton, Part I: Bony excrescences in skull base and upper extremity. Hell J Radiol 2020; 5(1): 28-37) we covered some common and some infrequent bony excrescences which may be clinically significant in the skull base and the upper extremity. The purpose of this second part is to overview bony excrescences and their associated clinical conditions in the lower extremity and pelvic bones.

1. Pelvis and hip joint

1.1. Hip joint

Femoroacetabular impingement results from abnormal contact between femur and acetabulum and is associated with pain and early degenerative changes in the hip joint. A recent consensus panel has defined this syndrome as "a motion-related clinical disorder of the hip with a triad of symptoms, clinical signs and imaging findings" [1-3].

The two intraarticular types of femoroacetabular impingement are "cam" and "pincer" types and in many patients a combination of the two may be observed. The "bump" at the anterolateral femoral head-neck junction, which is also called the "cam" or "pistol-grip" deformity, is observed as a bony outpouching of the femoral head, with the epiphyseal scar extending caudally and laterally into the femoral neck region **(Fig. 1)** [2, 3]. This bony protuberance at the femoral head-neck junction is reported in asymptomatic healthy individuals with high prevalence [4]. Thus it is recommended that, when present, it should be addressed as "cam morphology", to emphasise the fact that in the absence of relevant clinical findings, this morphologic feature alone does not constitute a diagnosis [1, 4].

1.2. Pelvis

Additional abnormal bony protuberances can be associated with hip impingement syndromes. Extraarticular impingement syndromes of the hip are the second most common cause for failed hip-preserving surgery requiring revision, following inadequate "cam" or "pincer" osteotomy [5]. Subspine impingement, one of the extraarticular forms, can clinically mimic femoroacetabular impingement, thus rendering imaging particularly important for accurate diagnosis [6-9].

An abnormally prominent anterior inferior iliac spine (AIIS) may cause bony impingement due to abnormal

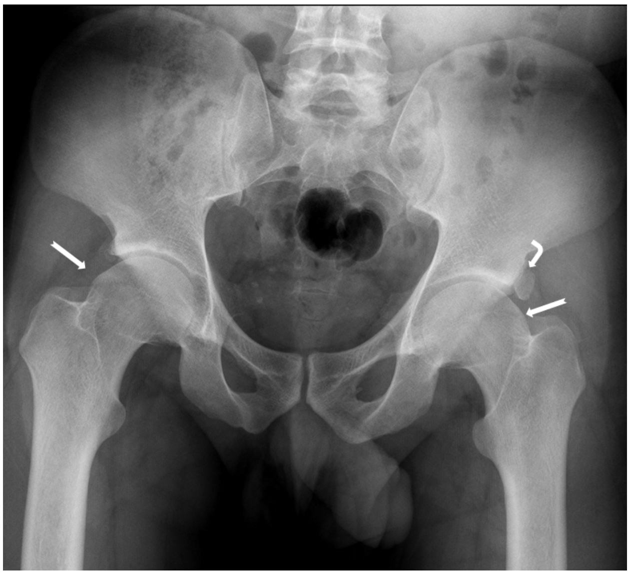

Fig. 1. *Anteroposterior pelvis radiograph of a 28-year-old male patient with clinical findings of femoroacetabular impingement syndrome on his right hip. Note that both femoral head-neck junctions demonstrate a "cam" morphology (arrows). A large os acetabulum (curved arrow) is present on the left side.*

contact with the femoral head or neck, during flexion, adduction and internal rotation of the hip, at a more distal location than the point of contact in cam or pincer femoroacetabular impingements [10]. This type of extraarticular hip impingement is called "subspine impingement".

Morphology of the AIIS has been shown to be significant in subspine impingement, where a prominent AIIS is associated with the highest risk [7].

Patients presenting with subspine impingement often report a previous avulsive trauma at the AIIS or affecting the rectus femoris muscle in their adolescence, possibly leading to progressive hypertrophic changes in the AIIS, resulting in an acquired prominent AIIS morphology **(Fig. 2)** [11-13]. This type of impingement and prominent AIIS morphology is especially common in football players [14]. AIIS may also be a site of enthesopathy in axial spondyloarthropathies, particularly juvenile spondyloarthropathy which may show the same clinical and imaging findings [15].

2. Knee

2.1. Distal femur and proximal tibia

2.1.1. Osteophytes

Although knee joint is one of the most commonly in-

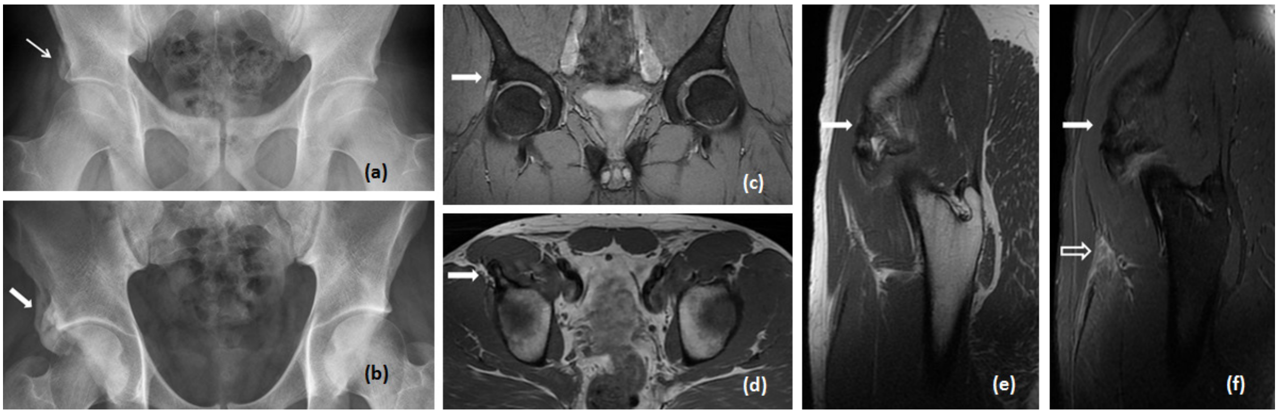

Fig. 2. *Anteroposterior radiographs of the pelvis from two different patients are shown. Right sided avulsion fracture of the anterior inferior iliac spine (AIIS) (arrow) is shown in the first patient (**a**), a 29-year-old recreational football player who reported a snapping sound together with a feeling of tearing at his right hip while shooting the ball. The second patient (**b**) is a 26-year-old professional football player with right sided hypertrophic AIIS (arrow). He was referred for imaging because of right hip pain during the game. His coronal gradient echo (**c**), axial (**d**) and sagittal (**e**) T1-weighted and sagittal fat suppressed PD-weighted (**f**) MR images are shown. Note that the AIIS on the right hip is substantially hypertrophic (arrows). Sagittal fs- PD image in (**f**) depicts a recent proximal rectus femoris muscle strain (open arrow).*

Fig. 3. *Anteroposterior left knee radiographs (**a, b**) of a 49-year-old female patient with 5 years interval (**a, b**) demonstrate the progression of osteophytes (arrows) in the lateral compartment and narrowing of joint space in the medial compartment over time. The loose body in the lateral compartment in her initial radiograph (open arrow in **a**) is displaced (not shown here) and not seen in the follow up imaging. Note that in the two coronal T1-weighted MR images obtained at the same time as the respective radiographs (**c, d**), the progression in osteophytes (white arrows), subchondral bone marrow changes (black arrows) and extrusion of medial meniscus (curved arrow) over time are more readily appreciated (**d**). Her initial knee MRI revealed a posterior root tear of the medial meniscus (not shown here).*

volved joints in osteoarthritis, it is beyond the scope of this article to review all aspects of the disease. However, given the high prevalence of knee involvement in osteoarthritis, the osteophytes at the knee joint are worth a brief caption here **(Fig. 3)**. They are frequently seen in patients over the age of 60 and most frequently in the medial compartment. Although they are the hallmarks of osteoarthritis, it should be noted that about 40% of the population with knee joint osteophytes are asymptomatic. Furthermore, progression of osteoarthritis is not affected by the size of osteophytes but, besides other factors, it is associated with malalignment of the knee joint [16-18].

2.1.2. Exostoses

Exostoses are the most frequent benign bony tumour-like

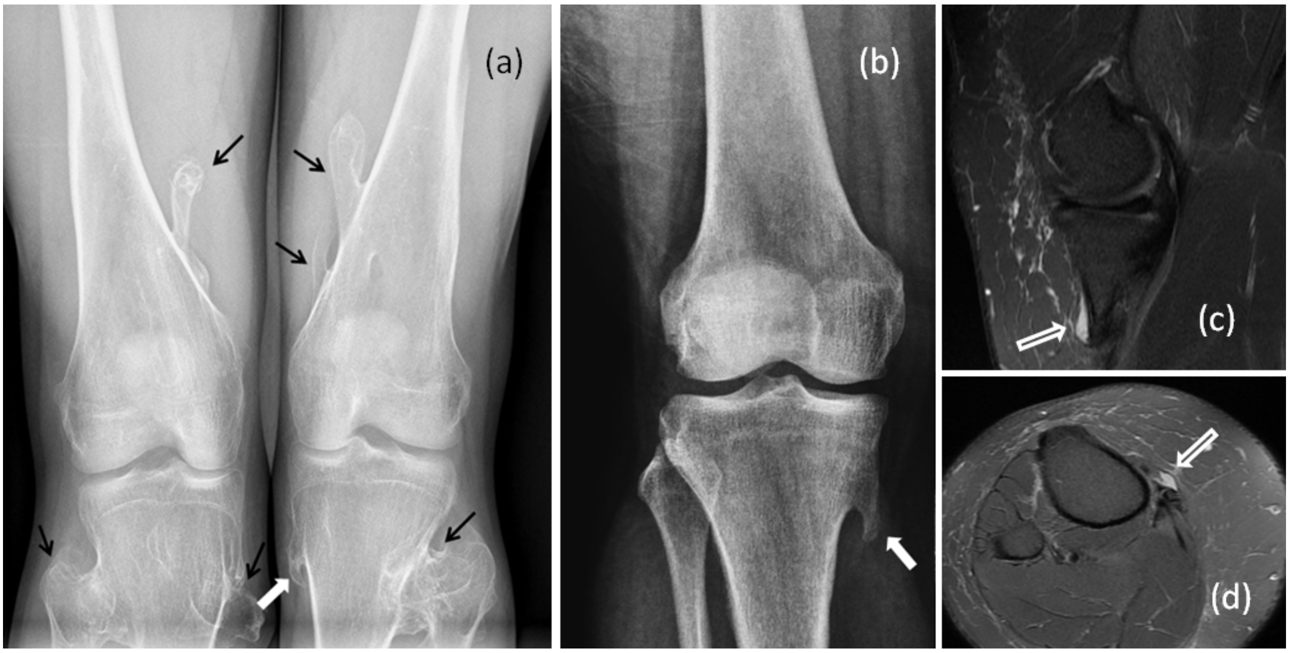

Fig. 4. *A 20-year-old male patient with hereditary multiple osteochondromatosis (**a**). There are numerous osteochondromas arising from the wide metaphyses at the distal femur and proximal tibia and fibula on both sides (black arrows). Note that on the left side, the medial osteochondroma at the proximal tibia resembles the solitary pes anserine exostosis (white thick arrows in **a** and **b**) in the 47-year-old female with pes anserine exostosis (arrow in **b**) and recurrent pes anserine bursitis (open arrow) which is appreciated in the sagittal fat suppressed T2-weighted (**c**) and axial fat suppressed proton density MR images (**d**).*

excrescences in long bones. In 4% of cases, solitary osteochondromas are seen around the knee joint [19-21]. Unless part of hereditary multiple exostoses syndrome **(Fig. 4a)**, which is also known as diaphyseal aclasia, osteochondromas are usually solitary [20].

Solitary exostoses of the pes anserinus tendon attachment site, also called pes anserine spurs, differ from typical osteochondromas as they do not have a cartilage cap **(Fig. 4)**. Due to their shape they have been referred to as "cloth hook exostosis" [22] with an "icicle" appearance in radiographs [23]. Thus, some researchers recommend the use of the name "pes anserine bony spurs" instead of osteochondromas for these lesions. Surgical resection is often limited to patients with pain despite the conservative measures [24].

2.1.3. Healed Segond fracture

Another bony bump that can be observed in the proximal tibia is the small osseous protuberance at its lateral aspect that develops as a result of a healed "Segond" fracture [25].

The relationship between the anterior cruciate ligament, meniscal tears and Segond fracture -the small avulsion fracture at the lateral capsular attachment site of proximal tibia- is well established in the literature [26-28]. However, when this fracture heals, a bony protuberance with a characteristic appearance **(Fig. 5)** can be observed on imaging studies. A healed Segond fracture may rarely mimic an osteophyte or an osteochondroma. However, direct relation to the articular surface of the tibia approximately 3-6 mm to the lateral tibial plateau and the parallel orientation to the joint, unlike an osteochondroma, are useful hints in recognising this bony bump [25].

A "reverse Segond" fracture, which represents avulsive injury of the deep capsular component of the medial collateral ligament, can be considered as a subtle bony fragment detached from the medial tibial condyle. This injury, like the Segond fracture, is associated with more severe soft tissue damage, particularly disruption of posterior cruciate ligament and medial meniscal tear. Similar to a healed Segond fracture, a healed reverse Segond fracture may potentially result in a bony bump at the edge of proximal medial tibial condyle [29].

2.1.4 Pellegrini-Stieda lesion

"Pellegrini-Stieda" lesion represents a post-traumatic

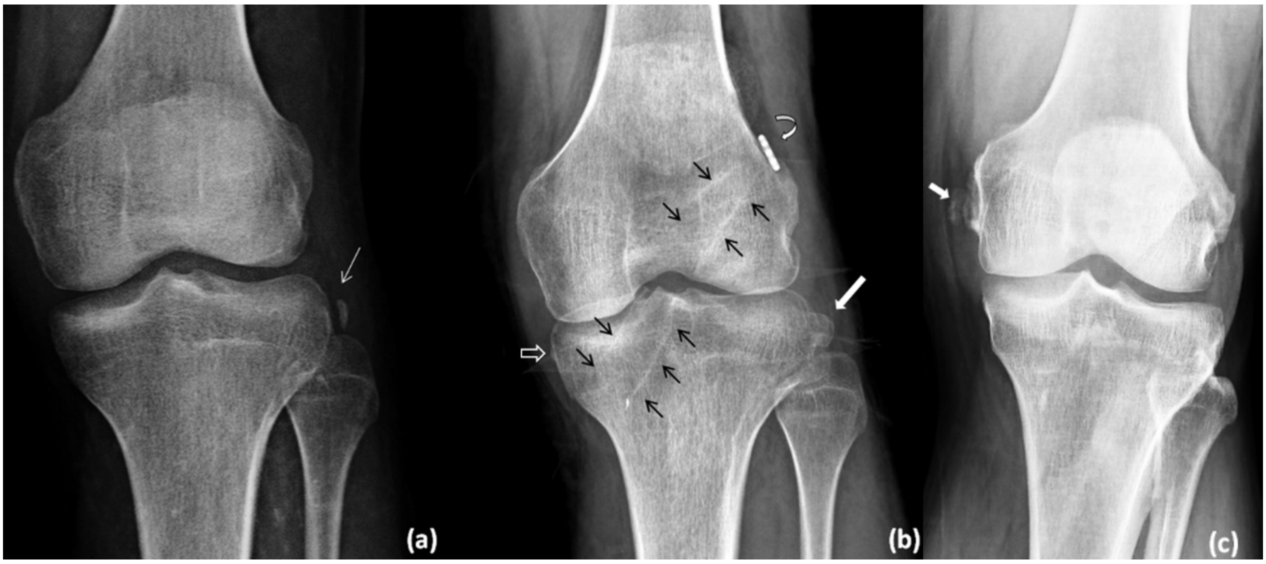

Fig. 5. *Anteroposterior knee radiograph of a 19-year-old male patient at his initial admission (**a**) after a knee injury during skiing shows the Segond fracture (arrow in **a**). Postoperative control radiograph at 8th month (**b**) after anterior cruciate ligament (ACL) reconstruction surgery demonstrates a bony bump on the lateral aspect of proximal tibia representing a healed Segond fracture (thick arrow in **b**). The tibial and femoral tunnels (black arrows) and endobutton (curved arrow) which is used to anchor the reconstructed ACL graft are clues to the patient's prior trauma and ACL reconstruction surgery. Note that, although the initial radiograph does not depict an avulsed fragment on the medial side of the proximal tibia, a slight bony irregularity has developed at the typical location of a reverse Segond fracture in the follow up radiograph (open arrow in **b**).The patient has sustained injury of the deep medial collateral ligament at its tibial attachment site (not shown here). In the anteroposterior knee radiograph of another patient with a history of knee injury 4 weeks ago (**c**) the Pellegrini- Stieda lesion is appreciated (arrow in **c**).*

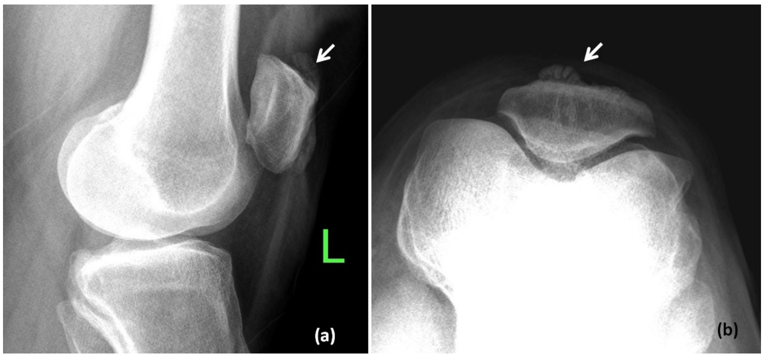

Fig. 6. *Lateral (**a**) and skyline (**b**) radiographs of the left knee in a 64-year-old male patient are shown. The enthesophyte at the upper pole of the patella (arrow in **a**) creates the "tooth" sign in the skyline view (arrow in **b**).*

ossification/calcification near the medial femoral condyle, secondary to injury of the medial collateral ligament or the tendon of the adductor magnus muscle **(Fig. 5c)**. This lesion is typically seen 3-4 weeks after knee trauma in patients of 25-40 years of age and more commonly in males. If pain accompanies the radiographic changes, then it is termed as "Pellegrini-Stieda" syndrome. Mendes et al. have described four patterns of ossification at this location and found that, depending on the structure that is involved (medial collateral ligament and/or distal adductor magnus tendon), the two particular types, "a beak-like appearance with an inferior orientation and femoral attachment" and "an elongated appearance with a superior orientation, parallel to the femur" may especially resemble exostotic bony lesions originating from the distal femur [30].

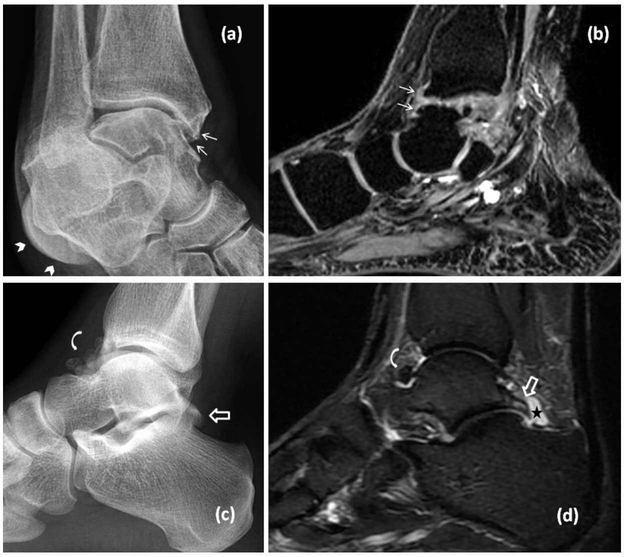

Fig. 7. *Mortise radiograph (**a**) and sagittal 3-D T2-weighted dual echo steady state water excitation MR image (**b**) of the right ankle of a 55-year-old female patient demonstrate anteromedial osteophytes at the opposing surfaces of tibia and talus (arrows). This patient was referred for a lateral sided soft tissue swelling (arrowheads in **a**) which turned out to be a ganglion cyst (not shown here). Anteromedial osteophytes at this location can also be seen in anteromedial ankle impingement syndrome, which is particularly common in kicking athletes. In another patient lateral radiograph (**c**) and short tau inversion recovery (STIR) image (**d**) of the ankle are shown. This 43-year-old male patient complains of crepitation and pain mostly at the posterior aspect of the ankle during running and playing football, compatible with posterior ankle impingement syndrome. The prominent Stieda process (open arrows) demonstrates bone marrow oedema on STIR image. Note that there is also effusion of the posterior subtalar recess (star) and soft tissue oedema around it. Multiple loose bodies in the anterior tibiotalar recess are also noted (curved arrows).*

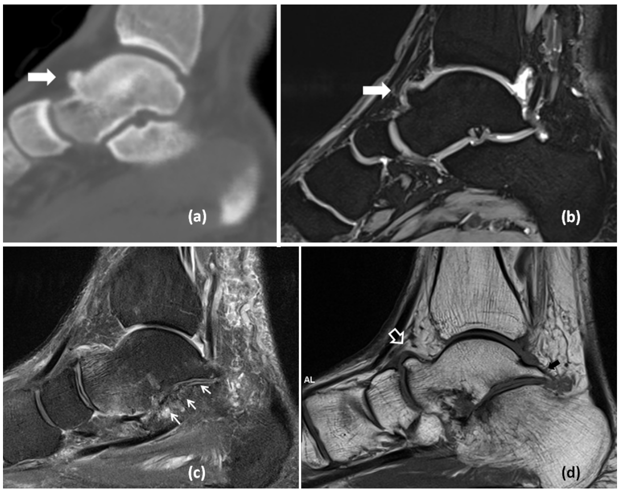

Fig. 8. *Hypertrophic talar ridge (thick arrows) is shown in the sagittal reformatted CT (**a**) and corresponding sagittal T2-weighted 3-D gradient echo images (**b**) of the right ankle of a 26-year-old professional football player. In another patient with fibrous coalition of the middle subtalar joint, associated degenerative changes (arrows) are shown on sagittal T2-weighted fat suppressed MR image (**c**). On T1-weighted image (**d**) the talar beak (open arrow) is observed at the superior margin of the talar head in this 64-year-old male patient. Note that he also has a prominent Stieda process on the posterior aspect of the talus (black arrow).*

2.1.5 Rare findings

Rarely, a hypertrophic medial tibial crest may result in the homonymous friction syndrome which is mostly seen in cyclists and shows soft tissue and subcortical bone marrow oedema ipsilaterally [31]. Another rare finding, which is demonstrated with bony outgrowth, is the presence of enthesophytes in patients with axial spondyloarthropahty and knee joint involvement. Younger patient age and locations such as posterior cruciate ligament, patellar tendon, iliotibial band insertion and joint capsule attachment sites, which are remote from the joint space, are hints in diagnosing these enthesophytes [32, 33].

2.2. Patella

2.2.1. Enthesophytes

Degenerative changes in the quadriceps tendon result in enthesophyte formation at the upper pole of the patella, where the tendon inserts. The new bone formation at the patellar insertion site can be readily appreciated on skyline knee radiographs as contour irregularity that was described as the patella “tooth” sign **(Fig. 6)** [34]. Although initially considered as a clinically insignificant radiographic finding, quadriceps tendon rupture in association with patellar “tooth” sign has been reported in later years [35].

3. Ankle and Foot

3.1. Talus

3.1.1. Osteophytes

Osteophytes are frequent in the ankle joint. They can be often found at the dorsal surface of the talus or navicular articular surface of the talar head, but also at the distal margin of the trochlea and anterior or anteromedial aspect of the tibia **(Fig. 7a-b)**. In athletes, particularly in football and rugby players, runners and ballet dancers, talar osteophytes may be associated with various ankle impingement syndromes. Anterior or anteromedial tibial and talar osteophytes are known to be associated with respective impingement syndromes, which are common causes of ankle pain particularly in patients younger than 40 years of age [36, 37].

The anterior impingement in which anterior osteophytes of tibia and talus are often present was first described as "athlete's ankle" [38]. These osteophytes are thought to arise after direct trauma. Patients with anterior impingement typically present with restriction of dorsiflexion and anterior joint pain [38-40].

3.1.2. Stieda process

Another excrescence of the talus is the elongated lateral tubercle of posterior process, also known as *Stieda process* **(Fig. 7c-d, Fig. 8d)**. With forced plantar flexion or repetitive episodes of plantar flexion, a prominent Stieda process can be associated with posterior ankle impingement. In this clinical entity, tenosynovitis or entrapment of flexor hallusis longus tendon and local synovitis result in irritation and posterior ankle pain [41]. The posterior impingement view radiograph, obtained by placing the medial side of the ankle against the detector with the ankle 25° externally rotated, provides better diagnostic performance in the evaluation of posterior ankle bony anatomy compared to standard lateral ankle radiographs [42].

3.1.3. Hypertrophic talar ridge

Another bony protuberance at the dorsal aspect of the talar neck is the hypertrophic talar ridge **(Fig. 8a-b)** which represents the enthesophytic change at the bony attachment sites of tibiotalar joint capsule and talonavicular ligament, about 7-14 mm distal to the trochlear articular surface. Hypertrophic talar ridge can also be found in the same group of athletes as well as in patients with diffuse idiopathic skeletal hyperostosis (DISH) [40, 43].

3.1.4. Talar beak

This particular triangular shaped bony excrescence of talus at its dorsal surface **(Fig. 8c-d)** is known to be associated with tarsal coalition, particularly at the middle subtalar joint [44]. It is postulated that talar beak arises due to excessive traction at the talonavicular joint by the abnormal subtalar joint kinematics. It is not clear if this beak is a unique outgrowth or one that represents an extreme talar ridge hypertrophy [43].

3.2. Calcaneus

3.2.1. Hypertrophic lateral calcaneal tubercle and retrotrochlear eminence

Hypertrophic lateral tubercle **(Fig. 9)**, also known as "peroneal tubercle" which can be seen in up to 30% of calcanei, may be associated with lateral ankle pain by causing stenosing peroneal tenosynovitis, peroneal tendon disorders and tears. Its aetiology is not clear and some authors suggest a congenital variation while others report previous trauma. For refractory cases, where symptomatic relief is not achieved conservatively, surgical resection of the bony tubercle can be performed [45, 46]. Another bony prominence just posterior to this tubercle is the retrotrochlear eminence of the calcaneus. Saupe et al. defined a cut-off height of 5 mm or more to define enlargement in both of these bony protruberances in the lateral side of the calcaneus [47].

3.2.2. Elongated anterior calcaneal process

Elongated anterior calcaneal process is seen in calcaneonavicular coalition, where an anomalous bony bar is present resembling an "anteater's nose" on lateral ankle views **(Fig. 10)** [48, 49]. Calcaneonavicular coalition is the most common type of tarsal coalition, followed by middle subtalar joint coalition [50]. This condition is best demonstrated on 45° internal oblique views. In addition to the anteater's nose sign, talar hypoplasia may indicate calcaneonavicular coalition [49, 51].

3.2.3. Calcaneal plantar enthesophytes

The plantar calcaneal enthesophyte **(Figs. 10a, 11a, 12a)**, a bony spur which is most commonly seen at the medial calcaneal tuberosity, can be associated with heel pain [52, 53]. Heel pain in the presence of a plantar cal-

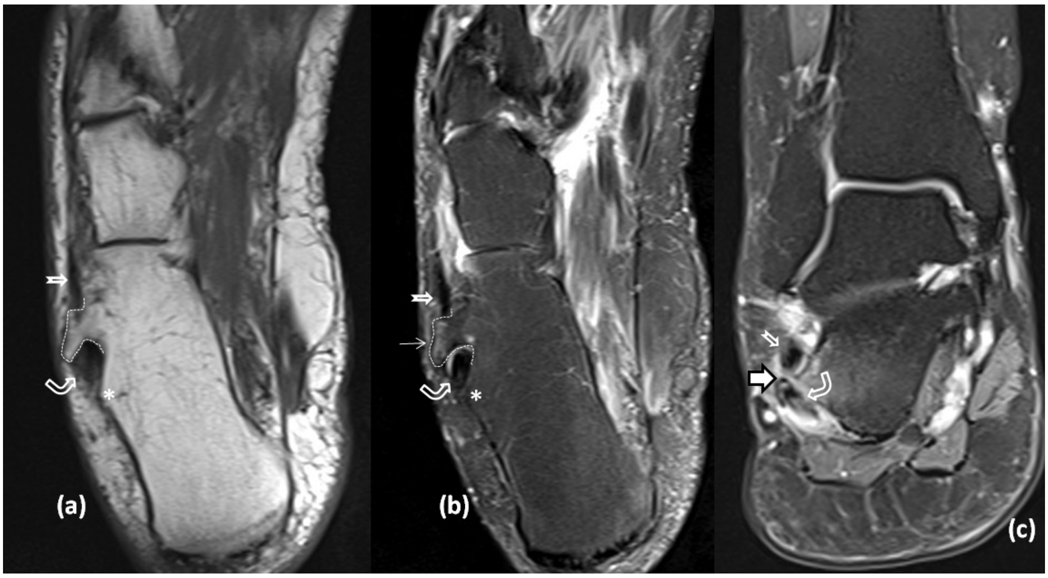

Fig. 9. *Hypertrophic peroneal tubercle of lateral calcaneus (dashed line) on T1-weighted (**a**) and fat suppressed T2-weighted (**b**) images of a 70-year-old male patient. The hook-like bony prominence is separating peroneus longus (curved arrow) and peroneus brevis (open arrow) tendons. Note the mild subcortical bone marrow oedema (thin arrow in **b**) in the hypertrophic peroneal tubercle. The retrocalceneal eminence (asterisk) lies posterior to the peroneal tubercle. In another 52-year-old female patient with lateral ankle pain, the prominent peroneal tubercle with its pointy tip (thick solid arrow) and accompanying bone marrow oedema are shown on this coronal fat suppressed proton density image (**c**). Note that in this patient there is tenosynovitis and partial thickness tear in the peroneus longus tendon (curved open arrow). The peroneus brevis tendon is normal (short open arrow).*

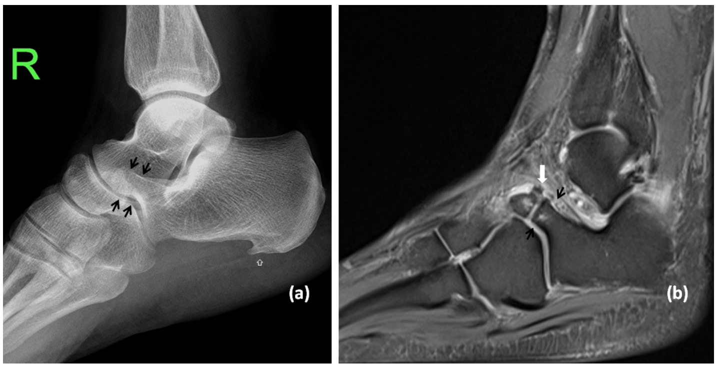

Fig. 10. *Lateral ankle radiograph (**a**) and sagittal fat suppressed proton density MR image (**b**) of a 53-year-old female patient with right ankle pain are presented. Note that the anterior process of the calcaneus that articulates with the navicular bone at the talonavicular coalition (thick white arrow) is elongated (black arrows), mimicking the nose of an anteater. Additionally a plantar calcaneal enthesophyte (white open arrow) is present. MR image shows degenerative changes involving both sides of the coalition (thick white arrow).*

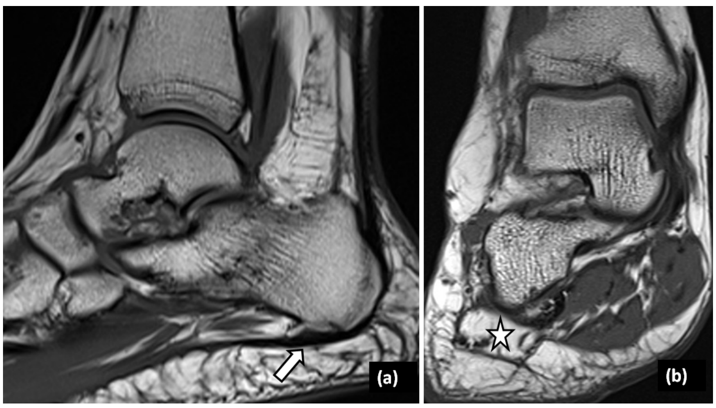

Fig. 11. *Sagittal (**a**) and coronal (**b**) T1-weighted images of a 41-year-old female patient with chronic heel pain are shown. The calcaneal spur at the inferior calcaneal process of plantar fascia insertion (arrow) and accompanying severe atrophy of adductor digiti minimi muscle (star in **b**) are compatible with Baxter's neuropathy.*

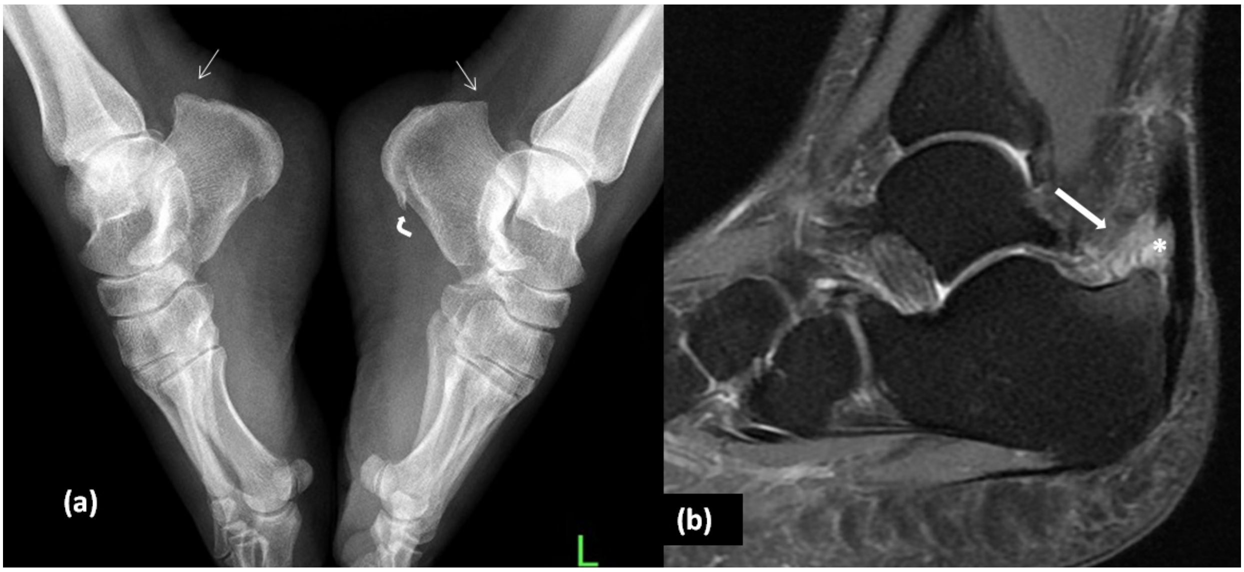

*Fig. 12. Lateral radiograph (**a**) of both feet of a 37-year-old female patient complaining of posterior ankle pain on the right side demonstrates bilateral Haglund deformity (arrows) and a calcaneal spur (curved arrow) on the left side. The sagittal STIR MR image of the right ankle (**b**) demonstrates the retrocalcaneal synovitis (thick arrow), associated bone marrow oedema at the superior aspect of the calcaneus and partial thickness tear (asterisk) at the distal Achilles tendon.*

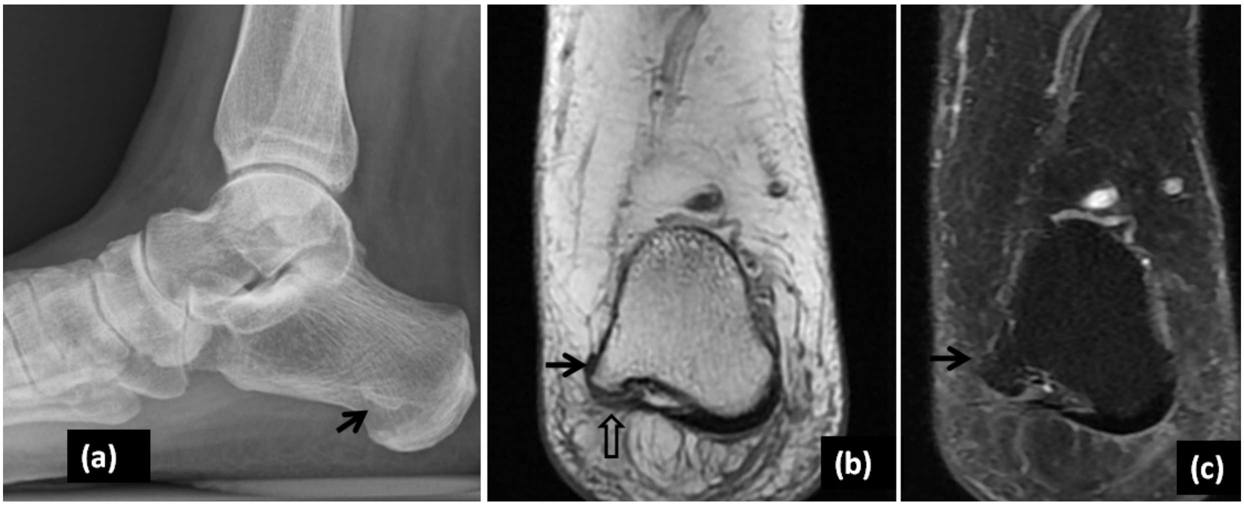

*Fig. 13. A 49-year-old female patient being investigated for medial sided right ankle pain presents with incidental finding of hypertrophic lateral plantar process of the calcaneal tuberosity (black arrows) on lateral ankle radiograph (**a**), coronal T1 (**b**) and STIR (**c**) MR images. Note that fibers of abductor digiti minimi originate from this bony prominence (open arrow).*

caneal enthesophyte is thought to be due to irritation or impingement of the medial or lateral plantar nerves or their branches [53-55]. Entrapment of the inferior calcaneal nerve, the first branch of lateral plantar nerve, can occur in the presence of large calcaneal enthesophytes and this painful clinical syndrome is called "Baxter neuropathy" **(Fig. 11)** [56]. Calcaneal plantar enthesophytes can be found at the insertion sites of abductor digiti minimi and flexor digitorum brevis muscles, deep to the plantar fascia, within the plantar fascia and at the insertion site of the short plantar ligament [53]. Mechanical alterations in the hindfoot causing a tug lesion, rheumatological disorders, mainly seronegative spondyloarthritides, DISH and ageing could be related

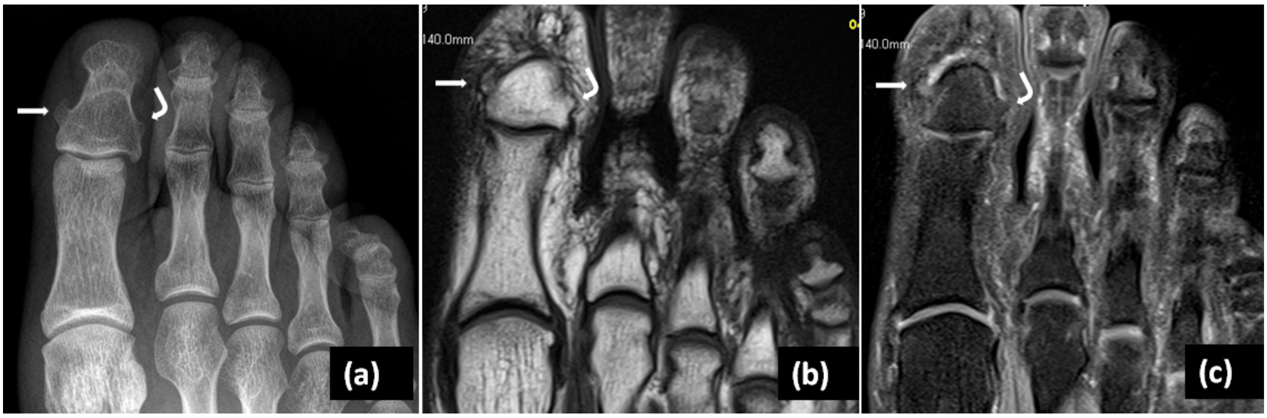

Fig. 14. *Enlarged views of anteroposterior radiograph of the left foot (**a**), axial T1-weighted (**b**) and postcontrast fat-suppressed T1-weighted (**c**) MR images showing medial (arrow) and lateral (curved arrow) exostosis of the distal phalanx at the base of the great toe in a 46-year-old female patient who complains of pain at this location. Note the slight enhancement at the medial exostosis on postcontrast fat suppressed axial T1-weighted image (**c**).*

Fig. 15. *Magnified posteroanterior radiograph (**a**) of the left foot of a 10-year-old female patient with pain and nail deformity on her great toe demonstrates a subungual osteochondroma (thick arrow), showing corticomedullary continuity with the distal phalanx. Corresponding axial STIR MR image demonstrates bone marrow oedema of the distal phalanx along with the subungual osteochondroma. Notice that the lesion has a thin and regular cartilage cap (thin arrows in **b**).*

to the development of plantar calcaneal enthesophytes [57-59]. The aetiology may not always be so clear-cut in calcaneal spurs but, when bony erosions together with whiskering and periosteal new bone at the insertion site of plantar aponeurosis are seen, these findings favour the diagnosis of spondyloarthritis, particularly reactive arthritis. In DISH and osteoarthritis, both of which are non-inflammatory conditions, no erosive bone changes are seen. In fact, these two disorders are where calcaneal spurs are most commonly reported, with the incidence of 91% and 81% respectively. Large, well-defined calcaneal spurs, lack of bony erosions and presence of Achilles or peroneal tendon calcifications at their insertion sites are useful tips to discriminate DISH from inflammatory conditions [60].

3.2.4. Haglund deformity

This common but poorly understood deformity of the posterior calcaneus has quite a lot synonyms such as retrocalcaneal exostosis, cucumber heel, prow beak deformity and "pump bump" [61]. Although the exact aetiology is not known, this deformity is more common in patients with altered foot biomechanics such as hindfoot varus and pes cavus, or those who wear low-back shoes, exerting chronic stress. It is more common in females and usually bilateral. In addition to this deformity, presence of soft tissue inflammation at the superficial bursa, Achilles tendon and retrocalcaneal bursa, leading to a painful posterior heel is known as Haglund syndrome [62, 63]. On lateral radiographs, the bony projection at the posterosuperior aspect of the calcaneus and loss of radiolucency in the retrocalcaneal recess can be seen. MRI can further elaborate the soft tissue changes such as retrocalcaneal and retro-Achilles bursae and bone marrow oedema at the calcaneal tuberosity **(Fig. 12)** [63].

3.2.5. Hypertrophic lateral plantar process of calcaneal tuberosity

The lateral intrinsic muscles of the foot anchor onto the lateral process of the calcaneal tuberosity. The lateral process is much smaller than the medial. However its size is found to be positively correlated with body mass index and the size of the peroneal tubercle [64]. A hypertrophic lateral process of the calcaneal tuberosity **(Fig. 13)** should not be confused with an exostosis.

3.3. Toes

3.3.1. Tuft exostosis

A more frequent but underappreciated great toe excrescence is the tuft exostosis at the medial or lateral aspects of the base of the distal phalanx **(Fig. 14)**. Having been addressed as an enthesophyte by some researchers, they are rarely associated with clinical findings, pain being the most common one if any. They have been observed more commonly in females and in patients with hallux valgus deformity which suggests a possible common aetiology or association with tight shoe-wear [65].

3.3.2. Subungual exostosis

The most well-known symptomatic bony protrusion of the distal phalanx of the great toe is a subungual exostosis. It presents as a firm swelling in the nail bed and can cause nail deformity, particularly in adolescence. Although it can be seen in any digit, the great toe is affected most commonly. On imaging, it is seen as a bony outgrowth taking origin from the dorsal aspect of the distal phalanx in the nail bed **(Fig. 15)**. In some cases, a thin cartilage cap covering the lesion may be observed, representing an osteochondroma variant [20, 66].

Discussion

This review summarises developmental and acquired bony protuberances in the lower extremity in the light of their clinical significance and imaging findings. Some of these lesions have been described on plain radiographs by earlier researchers but, with the increasing use of MRI and CT, their imaging findings on cross sectional imaging modalities and radiographs are recapped one more time.

Radiologists should be familiar with these bony excrescences and their imaging findings on different modalities in order not to mistake them for other pathologies. Furthermore, in some instances, being familiar with the clinical context that they are found, a single joint imaging can shed light to the underlying generalised or systemic disorders that the patients may be suffering from. R

Conflict of interest

The authors declared no conflicts of interest.

References

1. Griffin DR, Dickenson EJ, O'Donnell J, et al. The Warwick Agreement on femoroacetabular impingement syndrome (FAI syndrome): an international consensus statement. *Br J Sports Med* 2016; 50(19): 1169-1176.
2. Siebenrock KA, Wahab KH, Werlen S, et al. Abnormal extension of the femoral head epiphysis as a cause of cam impingement. *Clin Orthop Relat Res* 2004; (418): 54-60.
3. Ganz R, Parvizi J, Beck M, et al. Femoroacetabular impingement: a cause for osteoarthritis of the hip. *Clin Orthop Relat Res* 2003; (417): 112-120.
4. Dickenson E, Wall PD, Robinson B, et al. Prevalence of cam hip shape morphology: a systematic review. *Osteoarthritis Cartilage* 2016; 24(6): 949-961.
5. Ricciardi BF, Fields K, Kelly BT, et al. Causes and risk factors for revision hip preservation surgery. *Am J Sports Med* 2014; 42(11): 2627-2633.
6. Wong TT, Igbinoba Z, Bloom MC, et al. Anterior inferior iliac spine morphology: Comparison of symptomatic hips with femoroacetabular impingement and asymptomatic hips. *AJR Am J Roentgenol* 2019; 212(1): 166-172.
7. Hetsroni I, Poultsides L, Bedi A, et al. Anterior inferior iliac spine morphology correlates with hip range of motion: a classification system and dynamic model. *Clin Orthop Relat Res* 2013; 471(8): 2497-2503.
8. Blankenbaker DG, Tuite MJ. Non-femoroacetabular impingement. *Semin Musculoskelet Radiol* 2013; 17(3): 279-285.
9. Sutter R, Pfirrmann CW. Atypical hip impingement. *AJR Am J Roentgenol* 2013; 201(3): W437-442.
10. Larson CM, Kelly BT, Stone RM. Making a case for anterior inferior iliac spine/subspine hip impingement: three representative case reports and proposed concept. *Arthroscopy* 2011; 27(12): 1732-1737.
11. Matsuda DK, Calipusan CP. Adolescent femoroacetabular impingement from malunion of the anteroinferior iliac spine apophysis treated with arthroscopic spinoplasty. *Orthopedics* 2012; 35(3): e460-463.
12. Resnick JM, Carrasco CH, Edeiken J, et al. Avulsion fracture of the anterior inferior iliac spine with abundant reactive ossification in the soft tissue. *Skeletal Radiol* 1996; 25(6): 580-584.
13. Yildiz C, Yildiz Y, Ozdemir MT, et al. Sequential avulsion of the anterior inferior iliac spine in an adolescent long jumper. *Br J Sports Med* 2005; 39(7): e31.
14. Nawabi DH, Degen RM, Fields KG, et al. Anterior inferior iliac spine morphology and outcomes of hip arthroscopy in soccer athletes: A comparison to nonkicking athletes. *Arthroscopy* 2017; 33(4): 758-765.
15. Herregods N, Dehoorne J, Pattyn E, et al. Diagnositic value of pelvic enthesitis on MRI of the sacroiliac joints in enthesitis related arthritis. *Pediatr Rheumatol Online J* 2015; 13(1): 46.
16. Altman R, Asch E, Bloch D, et al. Development of criteria for the classification and reporting of osteoarthritis. Classification of osteoarthritis of the knee. Diagnostic and Therapeutic Criteria Committee of the American Rheumatism Association. *Arthritis Rheum* 1986; 29(8): 1039-1049.
17. Kellgren JH, Lawrence JS. Radiological assessment of osteo-arthrosis. *Ann Rheum Dis* 1957; 16(4): 494-502.
18. Zhang Y, Jordan JM. Epidemiology of osteoarthritis. *Clin Geriatr Med* 2010; 26(3): 355-369.
19. Kitsoulis P, Galani V, Stefanaki K, et al. Osteochondromas: review of the clinical, radiological and pathological features. *In Vivo* 2008; 22(5): 633-646.
20. Murphey MD, Choi JJ, Kransdorf MJ, et al. Imaging of osteochondroma: variants and complications with radiologic-pathologic correlation. *Radiographics* 2000; 20(5): 1407-1434.
21. Giudici MA, Moser RP Jr, Kransdorf MJ. Cartilaginous bone tumors. *Radiol Clin North Am* 1993; 31(2): 237-259.
22. Villiger KJ. ["Clothes-hook" exostosis]. [Article in German]. *Chirurg* 1974; 45(10): 480-482.
23. Ugai K, Sato S, Matsumoto K, et al. A clinicopathologic study of bony spurs on the pes anserinus. *Clin Orthop Relat Res* 1988; (231): 130-134.

24. Fraser RK, Nattrass GR, Chow CW, et al. Pes anserinus syndrome due to solitary tibial spurs and osteochondromas. *J Pediatr Orthop* 1996; 16(2): 247-248.
25. Bock GW, Bosch E, Mishra DK, et al. The healed Segond fracture: a characteristic residual bone excrescence. *Skeletal Radiol* 1994; 23(7): 555-556.
26. Dietz GW, Wilcox DM, Montgomery JB. Segond tibial condyle fracture: lateral capsular ligament avulsion. *Radiology* 1986; 159(2): 467-469.
27. Weber WN, Neumann CH, Barakos JA, et al. Lateral tibial rim (Segond) fractures: MR imaging characteristics. *Radiology* 1991; 180(3): 731-734.
28. Goldman AB, Pavlov H, Rubenstein D. The Segond fracture of the proximal tibia: a small avulsion that reflects major ligamentous damage. *AJR Am J Roentgenol* 1988; 151(6): 1163-1167.
29. Escobedo EM, Mills WJ, Hunter JC. The "reverse Segond" fracture: association with a tear of the posterior cruciate ligament and medial meniscus. *AJR Am J Roentgenol* 2002; 178(4): 979-983.
30. Mendes LF, Pretterklieber ML, Cho JH, et al. Pellegrini-Stieda disease: a heterogeneous disorder not synonymous with ossification/calcification of the tibial collateral ligament-anatomic and imaging investigation. *Skeletal Radiol* 2006; 35(12): 916-922.
31. Klontzas ME, Akoumianakis ID, Vagios I, et al. MR imaging findings of medial tibial crest friction. *Eur J Radiol* 2013; 82(11): e703-706.
32. McGonagle D, Gibbon W, O'Connor P, et al. Characteristic magnetic resonance imaging entheseal changes of knee synovitis in spondylarthropathy. *Arthritis Rheum* 1998; 41(4): 694-700.
33. Emad Y, Ragab Y, Bassyouni I, et al. Enthesitis and related changes in the knees in seronegative spondyloarthropathies and skin psoriasis: magnetic resonance imaging case-control study. *J Rheumatol* 2010; 37(8): 1709-1717.
34. Greenspan A, Norman A, Tchang FK. "Tooth" sign in patellar degenerative disease. *J Bone Joint Surg Am* 1977; 59(4): 483-485.
35. Hardy JR, Chimutengwende-Gordon M, Bakar I. Rupture of the quadriceps tendon: an association with a patellar spur. *J Bone Joint Surg Br* 2005; 87(10): 1361-1363.
36. Berberian WS, Hecht PJ, Wapner KL, et al. Morphology of tibiotalar osteophytes in anterior ankle impingement. *Foot Ankle Int* 2001; 22(4): 313-317.
37. Robinson P, White LM, Salonen D, et al. Anteromedial impingement of the ankle: using MR arthrography to assess the anteromedial recess. *AJR Am J Roentgenol* 2002; 178(3): 601-604.
38. Morris LH. Athlete's ankle. *J Bone Joint Surg Am* 1943; 25: 220.
39. Tol JL, van Dijk CN. Etiology of the anterior ankle impingement syndrome: a descriptive anatomical study. *Foot Ankle Int* 2004; 25(6): 382-386.
40. Berman Z, Tafur M, Ahmed SS, et al. Ankle impingement syndromes: an imaging review. *Br J Radiol* 2017; 90(1070): 20160735.
41. Aparisi Gomez MP, Aparisi F, Bartoloni A, et al. Anatomical variation in the ankle and foot: from incidental finding to inductor of pathology. Part I: ankle and hindfoot. *Insights Imaging* 2019; 10(1): 74.
42. Wiegerinck JI, Vroemen JC, van Dongen TH, et al. The posterior impingement view: an alternative conventional projection to detect bony posterior ankle impingement. *Arthroscopy* 2014; 30(10): 1311-1316.
43. Resnick D. Talar ridges, osteophytes, and beaks: a radiologic commentary. *Radiology* 1984; 151(2): 329-332.
44. Conway JJ, Cowell HR. Tarsal coalition: clinical significance and roentgenographic demonstration. *Radiology* 1969; 92(4): 799-811.
45. Burman M. Stenosing tendovaginitis of the foot and ankle; studies with special reference to the stenosing tendovaginitis of the peroneal tendons of the peroneal tubercle. *AMA Arch Surg* 1953; 67(5): 686-698.
46. Ochoa LM, Banerjee R. Recurrent hypertrophic peroneal tubercle associated with peroneus brevis tendon tear. *J Foot Ankle Surg* 2007; 46(5): 403-408.
47. Saupe N, Mengiardi B, Pfirrmann CW, et al. Anatomic variants associated with peroneal tendon disorders: MR imaging findings in volunteers with asymptomatic ankles. *Radiology* 2007; 242(2): 509-517.
48. Oestreich AE, Mize WA, Crawford AH, et al. The "anteater nose": a direct sign of calcaneonavicular coalition on the lateral radiograph. *J Pediatr Orthop* 1987; 7(6): 709-711.

49. Chapman VM. The anteater nose sign. *Radiology* 2007; 245(2): 604-605.
50. Stormont DM, Peterson HA. The relative incidence of tarsal coalition. *Clin Orthop Relat Res* 1983; (181): 28-36.
51. Sartoris DJ, Resnick DL. Tarsal coalition. *Arthritis Rheum* 1985; 28(3): 331-338.
52. Rubin G, Witten M. Plantar calcaneal spurs. *Am J Orthop* 1963; 5: 38-41.
53. Abreu MR, Chung CB, Mendes L, et al. Plantar calcaneal enthesophytes: new observations regarding sites of origin based on radiographic, MR imaging, anatomic, and paleopathologic analysis. *Skeletal Radiol* 2003; 32(1): 13-21.
54. Kopell HP, Thompson WA. Peripheral entrapment neuropathies of the lower extremity. *N Engl J Med* 1960; 262: 56-60.
55. Przylucki H, Jones CL. Entrapment neuropathy of muscle branch of lateral plantar nerve: a cause of heel pain. *J Am Podiatry Assoc* 1981; 71(3): 119-124.
56. Donovan A, Rosenberg ZS, Cavalcanti CF. MR imaging of entrapment neuropathies of the lower extremity. Part 2. The knee, leg, ankle, and foot. *Radiographics* 2010; 30(4): 1001-1019.
57. Resnick D, Feingold ML, Curd J, et al. Calcaneal abnormalities in articular disorders. Rheumatoid arthritis, ankylosing spondylitis, psoriatic arthritis, and Reiter syndrome. *Radiology* 1977; 125(2): 355-366.
58. Malhotra CM, Lally EV, Buckley WM. Ossification of the plantar fascia and peroneus longus tendons in diffuse idiopathic skeletal hyperostosis (DISH). *J Rheumatol* 1986; 13(1): 215-218.
59. McCarthy DJ, Gorecki GE. The anatomical basis of inferior calcaneal lesions. A cryomicrotomy study. *J Am Podiatry Assoc* 1979; 69(9): 527-536.
60. Sebes JI. The significance of calcaneal spurs in rheumatic diseases. *Arthritis Rheum* 1989; 32(3): 338-340.
61. Sella EJ, Caminear DS, McLarney EA. Haglund's syndrome. *J Foot Ankle Surg* 1998; 37(2): 110-114; discussion 173.
62. Pavlov H, Heneghan MA, Hersh A, et al. The Haglund syndrome: initial and differential diagnosis. *Radiology* 1982; 144(1): 83-88.
63. Lawrence DA, Rolen MF, Morshed KA, et al. MRI of heel pain. *AJR Am J Roentgenol* 2013; 200(4): 845-855.
64. Gill CM, Taneja AK, Bredella MA, et al. Osteogenic relationship between the lateral plantar process and the peroneal tubercle in the human calcaneus. *J Anat* 2014; 224(2): 173-179.
65. Montiel V, Alfonso M, Villas C, et al. Medial and lateral exostoses of the distal phalanx of the hallux: A potentially painful bunion-like structure. Part 1: Incidence and clinical application. *Foot Ankle Surg* 2019; 25(2): 158-164.
66. Garcia Carmona FJ, Pascual Huerta J, Fernandez Morato D. A proposed subungual exostosis clinical classification and treatment plan. *J Am Podiatr Med Assoc* 2009; 99(6): 519-524.

Ready - Made Citation

Akkaya Z, Şahin G. Beaks and peaks in adult skeleton, Part II: Bony excrescences in lower extremity. *Hell J Radiol 2020*; 5(2): 48-61.